

Effect of Dissolved Air on the Density and Refractive Index of Water

A. H. Harvey,^{1,2} S. G. Kaplan,³ and J. H. Burnett⁴

Received June 28, 2005

The effect of dissolved air on the density and the refractive index of liquid water is studied from 0 to 50°C. The density effect is calculated from the best available values of Henry's constants and partial molar volumes for the components of air; the results are in agreement with some previous experimental studies, but not others. The refractive-index effect is calculated as a function of wavelength from the same information, plus the refractivities of the atmospheric gases. Experimental measurements of the refractive-index effect are reported at both visible and ultraviolet wavelengths; the measured and calculated values are in reasonable agreement. The magnitude of the refractive-index change, while small, is several times larger than a previous estimate in the literature.

KEY WORDS: air; calibration; density; refractive index; water.

1. INTRODUCTION

Water, especially at atmospheric pressure near 25°C, is often used as a reference standard for thermophysical property measurements. For example, IUPAC [1] lists liquid water as a "recommended reference material" for density, surface tension, viscosity, thermal conductivity, heat capacity, relative permittivity, and refractive index. However, water in laboratory situations may be equilibrated with atmospheric air, whereas standard formulations for its properties are for air-free water. It is therefore useful to have

¹Physical and Chemical Properties Division, National Institute of Standards and Technology, 325 Broadway, Boulder, Colorado 80305-3328, U.S.A.

²To whom correspondence should be addressed. E-mail: aharvey@boulder.nist.gov

³Optical Technology Division, National Institute of Standards and Technology, 100 Bureau Drive, Stop 8442, Gaithersburg, Maryland 20899-8442, U.S.A.

⁴Atomic Physics Division, National Institute of Standards and Technology, 100 Bureau Drive, Stop 8424, Gaithersburg, Maryland 20899-8424, U.S.A.

an accurate knowledge of the effect of dissolved air on the properties of water.

The effect of dissolved air on the refractive index is part of a project on the optical properties of water in the ultraviolet [2] for immersion lithography, a new process where the use of water between the lens of a photolithography tool and a silicon wafer allows narrower lines to be drawn on computer chips [3]. The effect on the density is of interest in metrology and is a necessary intermediate step in modeling the refractive-index effect.

Several researchers [4–10] have measured the effect of dissolved air on the density of water, with mutually inconsistent results. Kell [11] attempted to model this effect based on the solubilities and partial molar volumes of individual atmospheric gases. Recent improvements in these underlying data offer the opportunity to improve significantly on Kell's calculations.

We are not aware of any quantitative study of the effect of dissolved air on the refractive index. In their definitive study of water's refractive index at visible wavelengths, Tilton and Taylor [12] stated that the effect of dissolved air should not exceed 1×10^{-6} in the index, which was approximately their experimental precision. For reasons to be discussed below (Section 6.3), we believe they were mistaken on this point.

In this work, we develop models for the effect of dissolved air on both the density and refractive index of liquid water. We also report measurements of the refractive-index effect.

2. CALCULATION OF AIR SOLUBILITY

The first step in calculating changes in density and refractive index due to dissolved air is to calculate the solubility of each component at standard atmospheric pressure. This calculation uses the standard composition of air and the thermodynamic Henry's constant for the solubility of each gas in water.

For the composition of dry air, we adopt the mole fractions given by Giacomo [13], which are appropriate for a laboratory setting. When trace components are omitted and the resulting mole fractions renormalized, the composition in Table I is obtained.

The Henry's constant is defined as an infinite-dilution limit:

$$k_{H,i} = \lim_{x_i \rightarrow 0} \left(\frac{f_i}{x_i} \right), \quad (1)$$

where f_i and x_i are the fugacity and mole fraction of solute i and $k_{H,i}$ is its (temperature-dependent) Henry's constant. Because we will be dealing with very low solubilities, Henry's law (assuming the proportionality

Table I. Composition of Model Air for this Work

Gas	Mole fraction
N ₂	0.78103
O ₂	0.20940
Ar	0.00917
CO ₂	0.00040

in Eq. (1) holds for finite x_i) will be adequate for our purposes. Calculations with a database for air properties [14] indicate that, at all conditions of interest in this study, the deviation of vapor-phase fugacities from ideality is negligible for our purposes. Therefore, we simplify our analysis by replacing f_i in Eq. (1) with p_i , the partial pressure of the solute gas. The solubility of each air component is then

$$x_i = \frac{p_i}{k_{H,i}}. \quad (2)$$

In recent years, improved experimental techniques have permitted the determination of Henry's constants with unprecedented accuracy for many gases in water. Results have been published by Rettich et al. for nitrogen [15], oxygen [16], and argon [17]. Their argon results are consistent with similar high-quality measurements by Krause and Benson [18], which we do not use here.

Rettich et al. expressed their measured Henry's constants with an equation of the form

$$\ln(k_{H,i}/1 \text{ Pa}) = a_{0,i} + a_{1,i}T^{-1} + a_{2,i}T^{-2}, \quad (3)$$

where T is the absolute temperature in kelvins. The temperature range varies for each solute; it begins near 0°C in each case and extends to about 40°C for Ar, 50°C for N₂, and 55°C for O₂. The coefficients of Eq. (3) for these solute gases are given in Table II.

The solubility of atmospheric carbon dioxide is more complicated. Aqueous CO₂ undergoes a weak ionization reaction, which can be written as



The second ionization to form CO₃²⁻ is negligible for our purposes, as is the amount of H⁺ due to the self-ionization of water. Harned and Davis

Table II. Parameters for Correlation of Henry's Constants in H₂O with Eqs. (3) and (6)

Solute	Ref.	a_0	a_1 (K)	a_2 (K ²)	a_3 (K ³)
N ₂	[15]	14.2766192	6.3866654×10^3	-1.1397892×10^6	–
O ₂	[16]	14.989460	5.742622×10^3	-1.070683×10^6	–
Ar	[17]	15.349542	5.467601×10^3	-1.029186×10^6	–
CO ₂	[20]	6.9809	1.2817×10^4	-3.7668×10^6	2.997×10^8

[19] determined the equilibrium constant $K = \frac{m_{\text{H}^+} m_{\text{HCO}_3^-}}{m_{\text{CO}_2}}$ (where m is the molality; the activity coefficients that should, strictly speaking, appear as corrections for nonideality can be taken as unity at the tiny concentrations of interest here) for reaction (4) from 0 to 50 °C and described it with the expression,

$$\log_{10} K = 14.8465 - 3404.71/T - 0.032786T. \quad (5)$$

Henry's constants for molecular CO₂ are taken from the critical evaluation by Carroll et al. [20]:

$$\ln(k_{\text{H}}/1 \text{ Pa}) = a_0 + a_1 T^{-1} + a_2 T^{-2} + a_3 T^{-3}, \quad (6)$$

where a_0 to a_3 are listed in Table II. After k_{H} is used in Eq. (2) to compute the amount of molecular CO₂ in solution, the equilibrium constant is used to calculate the ionic concentrations. At the conditions of interest in this study, the ionized form accounts for approximately 10–20% of the total CO₂ in solution.

With Henry's constants given by Eq. (3) for N₂, O₂, and Ar and by Eq. (6) for CO₂, and the CO₂ ionization reaction described by Eqs. (4) and (5), it is straightforward to calculate the equilibrium amount of each solute as a function of temperature and partial pressure. In this work, we consider a standard atmospheric total pressure of 101.325 kPa, which will include a contribution from water vapor (we make the equilibrium assumption that the air immediately adjacent to the water is at 100% relative humidity). While p_{w} , the equilibrium partial pressure of water vapor, is slightly affected by gas solubility in the liquid and by vapor-phase nonideality, these effects are negligible for our purposes and we take p_{w} as the vapor pressure of pure water, $p_{\text{w}}^{\text{sat}}$. Then, the partial pressure of each atmospheric gas is given by

$$p_i = y_i (101.325 \text{ kPa} - p_{\text{w}}^{\text{sat}}), \quad (7)$$

where y_i is the vapor-phase mole fraction from Table I and p_w^{sat} is computed as a function of temperature from the equation of Wagner and Pruss [21].

Table III gives the mole-fraction solubility of each solute at 5 K intervals for equilibrium with air at a total pressure of 101.325 kPa.

3. CALCULATION OF DENSITY EFFECT

3.1. Thermodynamic Formulation

The molar volume V_m of a mixture is the mole-fraction weighted sum of the partial molar volumes \bar{V}_i of the components:

$$V_m = \sum_{i=1}^n x_i \bar{V}_i. \quad (8)$$

For dilute solutions far from the solvent's critical point, the partial molar volume of the solvent (water) can be taken as its molar volume in the pure state, V_w , and the solute partial molar volumes are independent of concentration. Then we can write

$$V_m = x_w V_w + \sum_{i=2}^n x_i \bar{V}_i^\infty, \quad (9)$$

where x_w is the mole fraction of water, \bar{V}_i^∞ is the partial molar volume of solute i at infinite dilution, and the sum is over all solute species.

Table III. Equilibrium Solubilities of Atmospheric Gases in H₂O at 101.325 kPa Total Pressure, and Total Effect on Mass Density Calculated from Eq. (11)

t (°C)	$10^6 X_{N_2}$	$10^6 X_{O_2}$	$10^6 X_{Ar}$	$10^6 X_{CO_2}$	$10^6 X_{HCO_3^-}$	$\Delta\rho$ ($\mu\text{g} \cdot \text{cm}^{-3}$)
0	14.98	8.24	0.395	0.542	0.051	-4.69
5	13.20	7.19	0.345	0.453	0.050	-3.95
10	11.78	6.36	0.306	0.383	0.049	-3.34
15	10.63	5.68	0.274	0.326	0.047	-2.85
20	9.69	5.13	0.247	0.280	0.046	-2.44
25	8.91	4.67	0.225	0.242	0.044	-2.09
30	8.25	4.28	0.206	0.211	0.042	-1.79
35	7.68	3.94	0.190	0.185	0.041	-1.52
40	7.17	3.64	0.175	0.163	0.039	-1.29
45	6.72	3.38	0.163	0.144	0.037	-1.09
50	6.29	3.13	0.150	0.127	0.034	-0.90

3.2. Partial Molar Volumes

Measurements of partial molar volumes for dilute nitrogen, oxygen, and argon in water have been reported by Bignell [22] between 3 and 21 °C, and by Zhou and Battino [23] at 25 and 30 °C. We used our preferred Henry's constants [15–17] to recompute the \bar{V}_i^∞ of Bignell [22], whose original measurements were of the density change at saturated conditions at 101.325 kPa partial pressure; this in some cases shifted \bar{V}_i^∞ by about $0.1 \text{ cm}^3 \cdot \text{mol}^{-1}$ compared to Ref. 22, where older, less accurate Henry's constants [11] were used to convert the data. Figure 1 shows \bar{V}_i^∞ for N_2 and O_2 (data for Ar are omitted for clarity). The data of Bignell [22] (smooth curves) had a reproducibility (one standard deviation) of $0.18 \text{ cm}^3 \cdot \text{mol}^{-1}$ for N_2 and $0.10 \text{ cm}^3 \cdot \text{mol}^{-1}$ for O_2 ; no further uncertainty was given. Error bars for the data of Zhou and Battino [23] are estimated based on their statements about reproducibility and uncertainty.

Given the scatter shown in Fig. 1, it seems adequate to represent the partial molar volumes by a simple linear relationship, assigning an uncertainty large enough to cover both sets of results. Therefore, partial molar volumes were represented by

$$\bar{V}_i^\infty / (1 \text{ cm}^3 \cdot \text{mol}^{-1}) = b_0 + b_1 t, \quad (10)$$

where $t = T - 273.15$ is the Celsius temperature. Table IV gives the coefficients for Eq. (10). Equation (10) is also consistent with the older measurements of Tiepel and Gubbins [24] at 25 °C for O_2 and Ar. Based on the

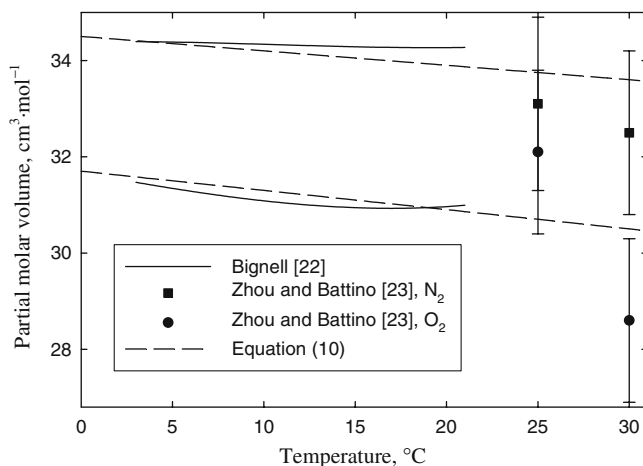


Fig. 1. Partial molar volumes for nitrogen and oxygen in water.

Table IV. Parameters for Correlating Partial Molar Volumes of Gases in H₂O with Eq. (10)

Solute	b_0	$b_1(^{\circ}\text{C}^{-1})$
N ₂	34.5	-0.03
O ₂	31.7	-0.04
Ar	32.7	-0.06
CO ₂	34.2	0

scatter and the range of temperatures covered, we assign an uncertainty for Eq. (10) of $1.5\text{ cm}^3\cdot\text{mol}^{-1}$ from 0 to 30°C and $2\text{ cm}^3\cdot\text{mol}^{-1}$ up to 50°C .

For the partial molar volume of CO₂, high-quality measurements have been reported at 25°C by two groups. Moore et al. [25] obtained $33.9\text{ cm}^3\cdot\text{mol}^{-1}$, and Hnědkovský et al. [26] obtained $34.4\text{ cm}^3\cdot\text{mol}^{-1}$. Since no data are available at other temperatures in our range of interest, we adopt a value of $34.2\text{ cm}^3\cdot\text{mol}^{-1}$, independent of temperature. While the consistency of these two studies is encouraging, we assign an uncertainty of $2\text{ cm}^3\cdot\text{mol}^{-1}$ due to the difficulty of the measurements and lack of knowledge of the temperature dependence.

We also consider the volumetric effect of the CO₂ ionization reaction, Eq. (4). At 25°C , the sum of the partial molar volumes of H⁺ and HCO₃⁻ (one can measure only electrically neutral combinations of ions) is known fairly accurately and has a value of $24.6\text{ cm}^3\cdot\text{mol}^{-1}$ [27], which we use at all temperatures. The uncertainty is small near 25°C ; the temperature dependence is not known but its maximum magnitude can be estimated based on data for other systems [28]. We assign an uncertainty of $1\text{ cm}^3\cdot\text{mol}^{-1}$ from 20 to 30°C and $3\text{ cm}^3\cdot\text{mol}^{-1}$ down to 0°C and up to 50°C .

The molar volume of pure water (at 101.325 kPa pressure) for use in Eq. (9) was obtained from the IAPWS formulation for thermodynamic properties of ordinary water [29] as implemented in a NIST database [30]. Since this quantity cancels to first order in the difference calculation of interest here, use of a different water density standard, such as that adopted by the CIPM from 0 to 40°C [31], would not affect our results.

3.3. Density Results

The effect of dissolved air on the molar density can be computed directly from Eq. (9) for the molar volume of the mixture V_m . This calculation requires the solubilities (Section 2) and partial molar volumes (Section 3.2) of each species. For metrology, the key quantity is the effect on the mass density, which is

$$\Delta\rho = \frac{M_m}{V_m} - \frac{M_w}{V_w}, \quad (11)$$

where M_m and M_w are the molar masses of the mixture (a mole-fraction weighted average of the individual-component molar masses) and of pure water, respectively. The last column of Table III contains calculated values of $\Delta\rho$.

In Fig. 2, we compare our values of $\Delta\rho$ with experimental results obtained in the last 50 years. Some older data, now only of historical interest, are discussed by Bignell [8]. The data of Bignell [8, 9], which were for 101.325 kPa partial pressure of dry air, were converted to 101.325 kPa total pressure by use of the vapor pressure of water [21]. For that study and the study of Watanabe and Iizuka [6, 7], the results were reported as equations rather than individual points; in those cases, the equations are plotted as smooth curves over the reported measurement range.

Our results agree very well with the measurements of Bignell [8, 9], with the single point measured by Lauder [4], and with all but one datum from Girard and Coarasa [10]. There is significant disagreement with the data of Watanabe and Iizuka [6, 7] and of Millero and Emmet [5].

The results of Kell [11], who used an approach similar to ours, are not shown in Fig. 2 because Kell's paper does not give enough information to reproduce his calculations. However, Fig. 2 can be compared to Fig. 3 of Kell's paper, and it is evident that his predicted values of $\Delta\rho$, while in the

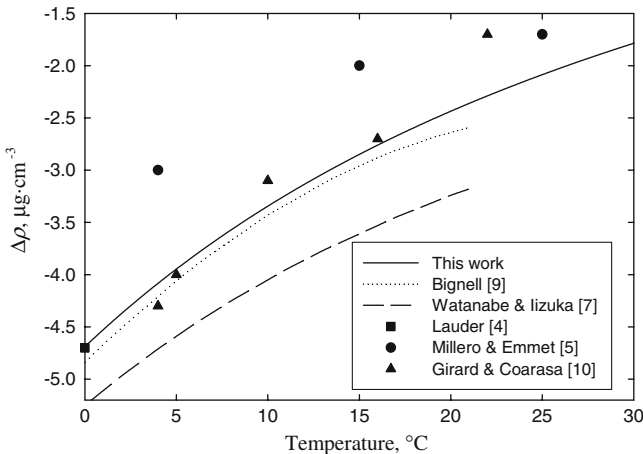


Fig. 2. Calculated and experimental values for $\Delta\rho$, the change in density of water upon equilibration with air at 101.325 kPa total pressure.

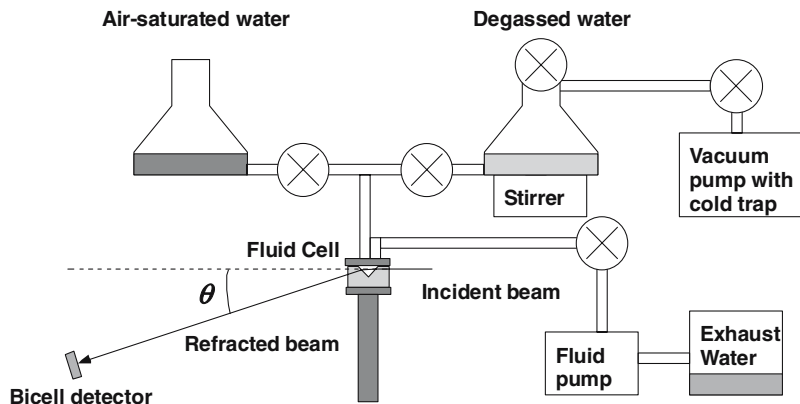


Fig. 3. Schematic diagram of the refractometer, vacuum, and fluid-handling apparatus used to measure the difference in refractive index between air-saturated and degassed water at several laser wavelengths, as described in the text.

same direction as those in this work, are smaller in magnitude by about $1.5 \mu\text{g} \cdot \text{cm}^{-3}$ at 0°C and larger in magnitude by about $0.6 \mu\text{g} \cdot \text{cm}^{-3}$ at 40°C , with the two results crossing near 20°C . The difference appears to be primarily due to different values for the partial molar volume of nitrogen. Kell used older results that had been derived indirectly from the pressure dependence of solubility; we believe those results are less reliable than the direct volumetric measurements employed in this work.

For convenience in metrology, an empirical equation was fitted to our results for $\Delta\rho$ as a function of temperature for air saturation of water at a total pressure of 101.325 kPa:

$$\Delta\rho/(\mu\text{g} \cdot \text{cm}^{-3}) = d_0 + d_1\tau^{-2.5} + d_2\tau^3, \quad (12)$$

where $\tau = t + 75$ with t the Celsius temperature. The fitted parameters are $d_0 = 0.103$, $d_1 = -2.371 \times 10^5$, and $d_2 = 1.820 \times 10^{-7}$. Equation (12) fits our calculated values of $\Delta\rho$ within $0.01 \mu\text{g} \cdot \text{cm}^{-3}$ from 0 to 50°C ; it should not be extrapolated outside this range.

4. ESTIMATION OF REFRACTIVE-INDEX EFFECT

4.1. Mixture Refractive-Index Formulation

For a pure component i , the refractive index n at molar density ρ_i is given by the Lorentz–Lorenz equation:

$$\frac{n^2 - 1}{n^2 + 2} = \frac{4\pi}{3} N_A \alpha_i \rho_i = A_i \rho_i, \quad (13)$$

where N_A is Avogadro's number and α_i is the molecular polarizability of species i .

At optical wavelengths, the refractive index reflects only electronic polarization, which is only slightly affected by intermolecular forces. Therefore, for a mixture we can write to a good approximation:

$$\frac{n^2 - 1}{n^2 + 2} = \sum_{i=1}^n A_i \rho_i = \rho_m \left(x_w A_w + \sum_{i=2}^n x_i A_i \right), \quad (14)$$

where ρ_m is the molar density of the mixture and the values of A_i are those for the pure solutes. To the extent that A_i varies with temperature, density, and wavelength for each solute, it is appropriate to evaluate each A_i if possible at the same conditions as the final mixture.

The change in refractive index due to dissolved air is then

$$\Delta n = n - n_w, \quad (15)$$

where n is the refractive index of the air-saturated mixture computed from Eq. (14), utilizing solubilities x_i from Section 2, the mixture molar density ρ_m from Section 3, and the component refractivities A_i as described below. n_w is the refractive index of pure water at the same temperature and pressure, computed from the IAPWS standard formulation [32].

4.2. Component Refractivities

For the solvent water, A_w is calculated from the IAPWS formulation [32] as a function of temperature, pressure, and wavelength. This utilizes the calculated refractive indices along with Eq. (13) and the IAPWS formulation [29, 30] for calculating density as a function of temperature and pressure. The refractive-index formulation [32] is based mainly on data at visible wavelengths, with larger uncertainties in the UV, and is not officially recommended for wavelengths shorter than 200 nm. However, recent work [2] has shown that it is still reasonably accurate at 193 nm. Small inaccuracies in A_w will mostly cancel in calculating Δn from Eq. (15).

For atmospheric gases, the refractivity has been determined accurately by Birch [33] at 632.99 nm. However, these gases exhibit sufficient dispersion at shorter wavelengths that use of Birch's values at ultraviolet conditions could introduce significant error. We therefore used additional data extending far into the UV for N_2 [34], O_2 [35], and CO_2 [36, 37], and covering a smaller range for Ar [38], which exhibits less dispersion. Data at wavelengths below 190 nm were not used, since that is roughly the limit of water's transparency. Refractivities extracted from these data were fitted

to a Sellmeier-type equation as a function of wavelength λ :

$$\frac{A_i}{A_0} = \frac{a_{1,i}}{a_{2,i} - (\lambda_0/\lambda)^2} + \frac{a_{3,i}}{a_{4,i} - (\lambda_0/\lambda)^2}, \quad (16)$$

where $A_0 = 1 \text{ cm}^3 \cdot \text{mol}^{-1}$, $\lambda_0 = 1000 \text{ nm}$, and a_1 through a_4 are adjustable parameters. The fits were constrained to reproduce the values from Birch [33] at 632.99 nm.

Table V contains the parameters for Eq. (16) for each atmospheric gas. The literature refractivities were fitted to better than 0.1% for N_2 and Ar and 0.2% for O_2 and CO_2 , which is sufficient for our purposes. For N_2 , Eq. (16) also agrees with the dispersion results of Peck and Khanna [39], which were not used in the fit.

Rather than estimate A_i for the H^+ and HCO_3^- ions, we assume that their sum is the same as the sum for the H_2O and CO_2 molecules. This is reasonable since the number of electrons is the same; the concentration of these ions is sufficiently small that a relatively large error in this assumption would have only a tiny impact on Δn .

4.3. Results

In Table VI, calculated values of Δn are tabulated at 5 K intervals for several different wavelengths, chosen for their common use in science and technology.

The Δn in Table VI can be thought of as resulting from a combination of two effects. The first is the change in molar density ρ_m due to dissolution of the gases. The second is the different (higher) values of A_i for the solute gases compared to water. These effects work in opposite directions, with the first being several times as large. For example, at 20°C and 632.99 nm, the molar density effect alone (if all the solute gases had the same A_i as water) would produce a value of -4.6×10^{-6} for Δn , and the

Table V. Parameters for Correlation of Refractivities of Air Components with Eq. (16)

Gas	a_1	a_2	a_3	a_4
N_2	23,541	25,493	509.43	147.13
O_2	29,631	10,846	63.047	51.173
Ar	20,351	9824.3	203.53	98.351
CO_2	9804.3	17,963	847.48	141.52

Table VI. Calculated Values of $10^6 \Delta n$ for Saturation of Water with Air at a Total Pressure of 101.325 kPa as a Function of Temperature at Selected Wavelengths

t ($^{\circ}\text{C}$)	193.39 nm	248.4 nm	365.015 nm	435.833 nm	589.3 nm	632.99 nm	1063.9 nm
0	-9.0	-7.3	-6.5	-6.3	-6.1	-6.1	-5.8
5	-7.8	-6.4	-5.6	-5.5	-5.3	-5.2	-5.0
10	-6.8	-5.6	-4.9	-4.8	-4.6	-4.6	-4.4
15	-6.1	-4.9	-4.3	-4.2	-4.1	-4.1	-3.9
20	-5.4	-4.4	-3.9	-3.8	-3.6	-3.6	-3.4
25	-4.9	-3.9	-3.5	-3.4	-3.3	-3.2	-3.1
30	-4.4	-3.6	-3.1	-3.1	-3.0	-2.9	-2.8
35	-4.0	-3.2	-2.9	-2.8	-2.7	-2.7	-2.5
40	-3.6	-2.9	-2.6	-2.5	-2.4	-2.4	-2.3
45	-3.3	-2.7	-2.4	-2.3	-2.2	-2.2	-2.1
50	-3.0	-2.4	-2.2	-2.1	-2.0	-2.0	-1.9

fact that the solutes have higher A_i than water produces a contribution to Δn of $+1.0 \times 10^{-6}$.

5. MEASUREMENTS OF REFRACTIVE INDEX EFFECT

5.1. Apparatus and Methodology

The measurements of refractive index differences were performed with a laser-based Hilger-Chance refractometer. This instrument has been described previously [40], and is shown schematically in Fig. 3.

The 90-degree inverted-prism fluid cell can be filled alternately with deionized water that has either been allowed to equilibrate with the surrounding air, or vigorously pumped and stirred to remove all residual dissolved gases to a partial pressure of approximately 1 Pa [41]. The temperature of the cell is controlled to 21.50°C , with 50 mK absolute uncertainty and 10 mK stability, by contact with a Cu sheath connected to a circulating thermally stabilized water bath and temperature feedback system. The Cu sheath also provides an O-ring vacuum seal at the top of the cell and feedthroughs to allow fluid ingress and egress. The temperature of the room air was approximately 20.5°C , and the atmospheric pressure typically between 99 and 100.5 kPa during the measurements.

The incident beam is from either a 633 nm continuous-wave HeNe laser, or a pulsed excimer laser operating at 248 or 193 nm (these are nominal wavelengths and were not measured in this work). The beam passes through a set of apertures and is normally incident on the front surface of the cell. The refracted beam is collected by a bicell position-sensitive

detector (two photodetectors separated by a thin gap) that has been calibrated to read angular deviation by rotating the detector arm to scan through the refracted beam while recording the bicell signal. It is found to produce a response that is linear in angular deviation over a range of $\pm 0.025^\circ$ from the center of the bicell, allowing accurate measurement of small angular differences. The beam is initially centered on the bicell, to produce nominally zero angular deviation signal.

Differential refractive-index data are acquired as follows:

- (a) Water from the air-saturated beaker is flowed through the system to fill the prism cell, the temperature is allowed to equilibrate for approximately 10 min, and then the angular deviation signal from the bicell is averaged for 10 min to produce a standard uncertainty in the mean value of approximately 3×10^{-5} degrees.
- (b) Degassed water from the evacuated beaker is flowed through the system and allowed to thermally equilibrate before the deviation signal is averaged again for 10 min.
- (c) The angular difference $\Delta\theta$ in the refracted beam between steps (a) and (b) is converted to Δn through two applications of the ideal Hilger-Chance formula [40]:

$$n_0 = \sqrt{n_p^2 - n_{\text{gas}} \sin(\theta)} \sqrt{n_p^2 - n_{\text{gas}}^2 \sin^2(\theta)}, \quad (17a)$$

$$\Delta n = \sqrt{n_p^2 - n_{\text{gas}} \sin(\theta + \Delta\theta)} \sqrt{n_p^2 - n_{\text{gas}}^2 \sin^2(\theta + \Delta\theta)} - n_0, \quad (17b)$$

where θ is the angle of the refracted beam with respect to the incident beam, n is the refractive index of the water sample, n_p is the refractive index of the prism material, and n_{gas} is the index of the surrounding air.

- (d) The cycle is repeated 3–5 times to determine the average value and standard uncertainty in Δn for each wavelength.

Equation (17) is accurate to within 0.1% for our prism cell, and any errors in Eq. (17) or in the measurement of θ will almost entirely cancel in calculating the difference Δn . In practice, the accuracy of $\Delta\theta$ is limited by thermal and mechanical drifts in the system to about 1×10^{-4} degrees, which corresponds to an uncertainty in Δn of approximately 1×10^{-6} .

5.2. Experimental Results

The measured differences between air-saturated and degassed water at three wavelengths are shown in Table VII. The values obtained for Δn are nearly identical at 633 and 248 nm, but clearly larger in magnitude at 193 nm.

Figure 4 compares the values of Δn predicted by the method of Section 4 with our experimental results at 21.5°C. The agreement is within the experimental uncertainty at two wavelengths; at 193 nm the prediction and experiment disagree, but just barely when one also considers the uncertainty in the model calculation as described in Section 6.1.

Table VII. Measured Values of $10^6 \Delta n$ for Saturation of Water with Air at 21.5°C

Wavelength (nm)	$10^6 \Delta n$
193	-6.7 ± 1
248	-4.3 ± 1
633	-4.4 ± 1

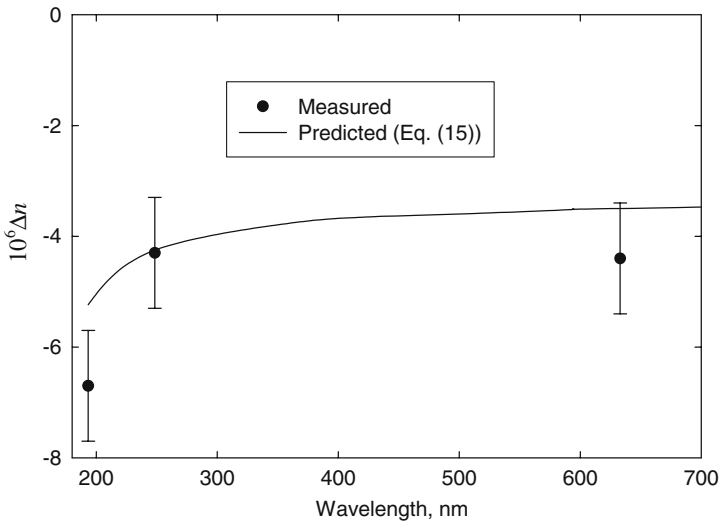


Fig. 4. Calculated and experimental values of Δn , the change in the refractive index of water upon equilibration with air at 21.5°C.

6. DISCUSSION

6.1. Uncertainties in Models

For the effect of dissolved air on the density, the only significant uncertainties are the partial molar volumes of nitrogen and oxygen. The contributions from uncertainties in Henry's constants for the solute gases and in the partial molar volumes of the minor air constituents and CO₂ ionization products are smaller by more than one order of magnitude.

When the uncertainties in \bar{V}_i^∞ of N₂ and O₂ discussed in Section 3.2 are propagated through the density calculations, they result in the changes in $\Delta\rho$ shown in Table VIII. The temperature variation in Table VIII is a result of the decrease in solubility of the gases with increasing temperature, and of the increased uncertainty of \bar{V}_i^∞ at the two highest temperatures. Under the assumption that these are independent contributions, the resulting combined uncertainty in $\Delta\rho$ is given in the last column of Table VIII. This assumption of independence is questionable, since the same data sources for \bar{V}_i^∞ were used for both gases. Therefore, the last column in Table VIII may be an underestimate; an upper bound on the total uncertainty would be obtained by adding the first two columns.

The uncertainty in Δn is again dominated by the partial molar volumes of N₂ and O₂; the uncertainties in the refractivities of the gases (A_i) are relatively small, and the difference calculation is largely insensitive to any uncertainty in water's refractivity A_w .

The effect on Δn of the uncertainties in \bar{V}_i^∞ was estimated by propagating them through the calculations in the same manner as for $\Delta\rho$. The resulting contributions for N₂ and O₂ and their combined uncertainty (again assuming the effects are independent; see above for a caveat about that assumption) are listed in Table IX for two wavelengths. It is noteworthy that the relative uncertainty due to \bar{V}_i^∞ is less for Δn than for $\Delta\rho$; this is because $\Delta\rho$ results from relatively small (and therefore sensitive to

Table VIII. Uncertainty in $\Delta\rho$ ($\mu\text{g}\cdot\text{cm}^{-3}$) due to Uncertainty in Partial Molar Volumes for N₂ and O₂

t (°C)	N ₂ contribution	O ₂ contribution	Combined N ₂ and O ₂
0	1.25	0.69	1.42
10	0.98	0.53	1.11
20	0.80	0.43	0.91
30	0.68	0.35	0.77
40	0.78	0.40	0.88
50	0.68	0.34	0.76

uncertainties in \overline{V}_i^∞) changes in *mass* density due to dissolved gases, while Δn is due to the change in *molar* density, which is a more pronounced effect.

A possible source of systematic error for Δn is the implicit assumption in Eq. (14) that the refractivities of water and the solutes are unaffected by mixing. While refractivities are relatively insensitive to molecular environment, suggesting that mixing effects should be small, we know of no way to quantitatively assess the accuracy of this assumption. The overall agreement with experiment shown in Fig. 4 suggests that the assumption is reasonable, although the modest disagreement at 193 nm might be a sign that it is less accurate at short wavelengths where water begins to exhibit some absorption.

6.2. Effect of Changing Atmospheric Conditions

The model results presented here are for a total atmospheric pressure of 101.325 kPa, which will not always be the case in real situations. Because $\Delta\rho$ and Δn are both directly proportional to the amount of dissolved air, which in turn is proportional to its partial pressure (except for a negligibly small nonlinearity due to CO_2 dissociation), our results can be scaled to other atmospheric pressures by multiplying by the ratio of the partial pressure of air (excluding its water content) at total pressure p to that at the standard pressure $p_0 = 101.325$ kPa:

$$\frac{(\Delta\rho)_p}{(\Delta\rho)_{p_0}} = \frac{(\Delta n)_p}{(\Delta n)_{p_0}} = \frac{p - p_w^{\text{sat}}}{p_0 - p_w^{\text{sat}}}, \quad (18)$$

where p_w^{sat} is the vapor pressure of water at the temperature of interest [21].

Table IX. Uncertainty in $10^6\Delta n$ due to Uncertainty in Partial Molar Volumes for N_2 and O_2

t ($^\circ\text{C}$)	193.39 nm			632.99 nm		
	N_2	O_2	Combined	N_2	O_2	Combined
0	0.62	0.35	0.72	0.46	0.25	0.52
10	0.49	0.27	0.56	0.36	0.19	0.41
20	0.40	0.22	0.46	0.29	0.15	0.33
30	0.34	0.18	0.38	0.24	0.13	0.28
40	0.39	0.20	0.44	0.29	0.15	0.33
50	0.34	0.17	0.38	0.25	0.13	0.28

One can also consider the effect of changing composition of dry air; normally, the only significant variability in laboratory air is the CO₂ content, which is affected by respiration and other anthropogenic sources. The standard practice is to consider any change in the mole fraction of CO₂ to be accompanied by an equal and opposite change in that of O₂. We can consider the effect of such a change in the air composition given in Table I.

If the mole fraction of CO₂ is increased from 0.0004 to 0.0005 (with a corresponding decrease in O₂), the computed values of $\Delta\rho$ are less negative by an amount ranging from 0.09 $\mu\text{g}\cdot\text{cm}^{-3}$ at 0°C to 0.03 $\mu\text{g}\cdot\text{cm}^{-3}$ at 50°C. These changes are small compared to the uncertainties in Table VIII. The effect of such a change in atmospheric CO₂ on Δn is negligible over the conditions of this study, never exceeding 10^{-8} .

It has recently been suggested [42, 43] that the mole fraction of argon in the standard composition of dry air [13] is slightly too small (and that of nitrogen too large). If this is confirmed and a new standard air composition adopted, the values in Table I could be replaced and the calculations repeated. Sample calculations indicate that the changes in both $\Delta\rho$ and Δn due to such a change would be negligible compared to other uncertainties.

6.3. Insight into Early NBS Work

The painstaking work of Tilton and Taylor [12] is considered definitive for the refractive index of liquid water at visible wavelengths from 0 to 60°C. While they did not apply modern uncertainty analysis, the precision of their measurements was better than 1×10^{-6} in the index, and they suggest that possible systematic errors did not exceed 1×10^{-6} .

However, we believe their analysis of the effect of dissolved gases (Section VI.3 of their paper [12]) was inadequate. The water for their experiments came directly from a house still and was probably initially air-free. It was used without further degassing, but with efforts made to limit contact with air.

Tilton and Taylor mention preliminary experiments where “... *some-what higher indices of stored distilled water were obtained after heating and degassing. The amount of this increase was not accurately measured but in some cases the increase at room temperatures exceeded 5×10^{-6} .*” An increase of this magnitude upon degassing of air-saturated water is consistent with our results (see Tables VI and VII). However, Tilton and Taylor dismissed the effect of air on the index, quoting a formula relating relative changes in refractive index and density, which in our notation reads

$$\frac{\Delta n}{n} = \frac{1}{3} \frac{\Delta\rho}{\rho}. \quad (19)$$

Since the relative change in water's mass density upon saturation with air was thought to be about -3×10^{-6} (which is approximately correct near 20°C ; see Fig. 2), they concluded that the effect "should not exceed 1×10^{-6} in index."

However, Eq. (19) applies (approximately) only to a fluid of fixed composition, where ρ is altered by a change in temperature or pressure. It is *not* applicable to changes caused by varying composition. One can easily see this by a thought experiment in which D_2O is added to pure H_2O ; the mass density would change significantly but there would be little effect on the refractive index. Therefore, their claim about the effect of air saturation on water's refractive index was unfounded.

Because Tilton and Taylor (perhaps given false assurance by the incorrect use of Eq. (19)) did not verify whether their efforts to keep their samples free of dissolved air were successful, it is possible that their measurements were on water partially saturated with air. Therefore, we believe their data should be considered to have an additional uncertainty component of approximately the magnitude of the effect derived in Section 4.

6.4. Impact on IAPWS Formulation

Because the data of Tilton and Taylor [12] were a key source for the formulation of the refractive index of water adopted by the International Association for the Properties of Water and Steam (IAPWS) [32], the question arises whether the additional uncertainty in these data affects this formulation. Because IAPWS used a relatively simple equation to cover a wide range of conditions, the formulation does not fit the Tilton and Taylor data within their reported uncertainties. The uncertainty that IAPWS assigns to its formulation in this region is 1.5×10^{-5} . Because the newly recognized uncertainty in the Tilton and Taylor data due to possible air content is on the order of 5×10^{-6} , the existing uncertainty estimate for the IAPWS formulation appears to be adequate.

7. CONCLUSIONS

We have developed a model for the effect of dissolved atmospheric air on the density of liquid water from 0 to 50°C . While experimental data for this quantity are inconsistent among different investigators, our results are in good agreement with several of the sources. Our model also covers a temperature range wider than that of the experimental measurements, which only extend to 25°C .

We have also calculated the effect of dissolved air on the refractive index of water, and validated our model with the first quantitative

measurements of this effect. Good agreement is obtained between the measurements and the model, although the agreement appears to deteriorate somewhat at the shortest ultraviolet wavelength investigated. The magnitude of the refractive-index effect is on the order of 5×10^{-6} , several times larger than had been previously asserted [12] but still small for most purposes. For the application of immersion lithography, this effect is of marginal significance; some care may be needed to avoid large gradients or sudden changes in the dissolved air content.

ACKNOWLEDGMENTS

We thank A. Anderko and A. V. Plyasunov for discussions on data for partial molar volumes, N. Bignell for clarification of some issues related to Refs. 8, 9, and 22, R. S. Davis for information concerning Ref. 10, D. G. Archer for discussions on degassing and related issues, and E. W. Lemmon for assistance in developing Eq. (12). Partial financial support for this work was provided by International Sematech.

REFERENCES

1. International Union of Pure and Applied Chemistry, *Recommended Reference Materials for the Realization of Physicochemical Properties*, K. N. Marsh, ed. (Blackwell Scientific, New York, 1987).
2. J. H. Burnett and S. G. Kaplan, *J. Microlith. Microfab. Microsys.* **3**:68 (2004).
3. B. Smith, *OE Magazine* **4**(7):22 (July 2004).
4. I. Lauder, *Aust. J. Chem.* **12**:40 (1959).
5. F. J. Millero and R. T. Emmet, *J. Mar. Res.* **34**:15 (1976).
6. H. Watanabe and K. Iizuka, *Jpn. J. Appl. Phys.* **20**:1979 (1981).
7. H. Watanabe and K. Iizuka, *Metrologia* **21**:19 (1985) [Erratum: *ibid.* **22**:115 (1986)].
8. N. Bignell, *Metrologia* **19**:57 (1983).
9. N. Bignell, *Metrologia* **23**:207 (1986/87).
10. G. Girard and M.-J. Coarasa, in *Precision Measurement and Fundamental Constants II*, NBS Special Publication 617, B. N. Taylor and W. D. Phillips, eds. (U.S. Government Printing Office, Washington, 1984), p. 453.
11. G. S. Kell, *J. Phys. Chem. Ref. Data* **6**:1109 (1977).
12. L. W. Tilton and J. K. Taylor, *J. Res. Nat. Bur. Stand.* **20**:419 (1938).
13. P. Giacomo, *Metrologia* **18**:33 (1982).
14. E. W. Lemmon, M. O. McLinden, and M. L. Huber, *Reference Fluid Thermodynamic and Transport Properties*, NIST Standard Reference Database 23, Version 7.0 (National Institute of Standards and Technology, Gaithersburg, Maryland, 2002).
15. T. R. Rettich, R. Battino, and E. Wilhelm, *J. Solution Chem.* **13**:335 (1984).
16. T. R. Rettich, R. Battino, and E. Wilhelm, *J. Chem. Thermodyn.* **32**:1145 (2000).
17. T. R. Rettich, R. Battino, and E. Wilhelm, *J. Solution Chem.* **21**:987 (1992).
18. D. Krause and B. B. Benson, *J. Solution Chem.* **18**:823 (1989).
19. H. S. Harned and R. Davis, Jr., *J. Am. Chem. Soc.* **65**:2030 (1943).

20. J. J. Carroll, J. D. Slupsky, and A. E. Mather, *J. Phys. Chem. Ref. Data* **20**:1201 (1991).
21. W. Wagner and A. Pruss, *J. Phys. Chem. Ref. Data* **22**:783 (1993).
22. N. Bignell, *J. Phys. Chem.* **88**:5409 (1984).
23. T. Zhou and R. Battino, *J. Chem. Eng. Data* **46**:331 (2001).
24. E. W. Tiepel and K. E. Gubbins, *J. Phys. Chem.* **76**:3044 (1972).
25. J. C. Moore, R. Battino, T. R. Rettich, Y. P. Handa, and E. Wilhelm, *J. Chem. Eng. Data* **27**:22 (1982).
26. L. Hnědkovský, R. H. Wood, and V. Majer, *J. Chem. Thermodyn.* **28**:125 (1996).
27. E. L. Shock and H. C. Helgeson, *Geochim. Cosmochim. Acta* **52**:2009 (1988).
28. Y. Marcus, *Ion Properties* (Marcel Dekker, New York, 1997).
29. W. Wagner and A. Pruß, *J. Phys. Chem. Ref. Data* **31**:387 (2002).
30. A. H. Harvey, A. P. Peskin, and S. A. Klein, *NIST/ASME Steam Properties*, NIST Standard Reference Database 10, Version 2.2 (National Institute of Standards and Technology, Gaithersburg, Maryland, 2000).
31. M. Tanaka, G. Girard, R. Davis, A. Peuto, and N. Bignell, *Metrologia* **38**:301 (2001).
32. A. H. Harvey, J. S. Gallagher, and J. M. H. Levelt Sengers, *J. Phys. Chem. Ref. Data* **27**:761 (1998).
33. K. P. Birch, *J. Opt. Soc. Am. A* **8**:647 (1991).
34. U. Griesmann and J. H. Burnett, *Opt. Lett.* **24**:1699 (1999).
35. P. L. Smith, M. C. E. Huber, and W. H. Parkinson, *Phys. Rev. A* **13**:1422 (1976).
36. J. G. Old, K. L. Gentili, and E. R. Peck, *J. Opt. Soc. Am.* **61**:89 (1971).
37. A. Bideau-Mehu, Y. Guern, R. Abjean, and A. Johannin-Gilles, *Opt. Commun.* **9**:432 (1973).
38. E. R. Peck and D. J. Fisher, *J. Opt. Soc. Am.* **54**:1362 (1964).
39. E. R. Peck and B. N. Khanna, *J. Opt. Soc. Am.* **56**:1059 (1966).
40. S. G. Kaplan and J. H. Burnett, *Appl. Opt.*, in press.
41. R. Battino, M. Banzhof, M. Bogan, and E. Wilhelm, *Anal. Chem.* **43**:806 (1971).
42. S. Y. Park, J. Y. Kim, J. B. Lee, M. B. Esler, R. S. Davis, and R. I. Wielgosz, *Metrologia* **41**:387 (2004).
43. A. Picard, H. Fang, and M. Gläser, *Metrologia* **41**:396 (2004).